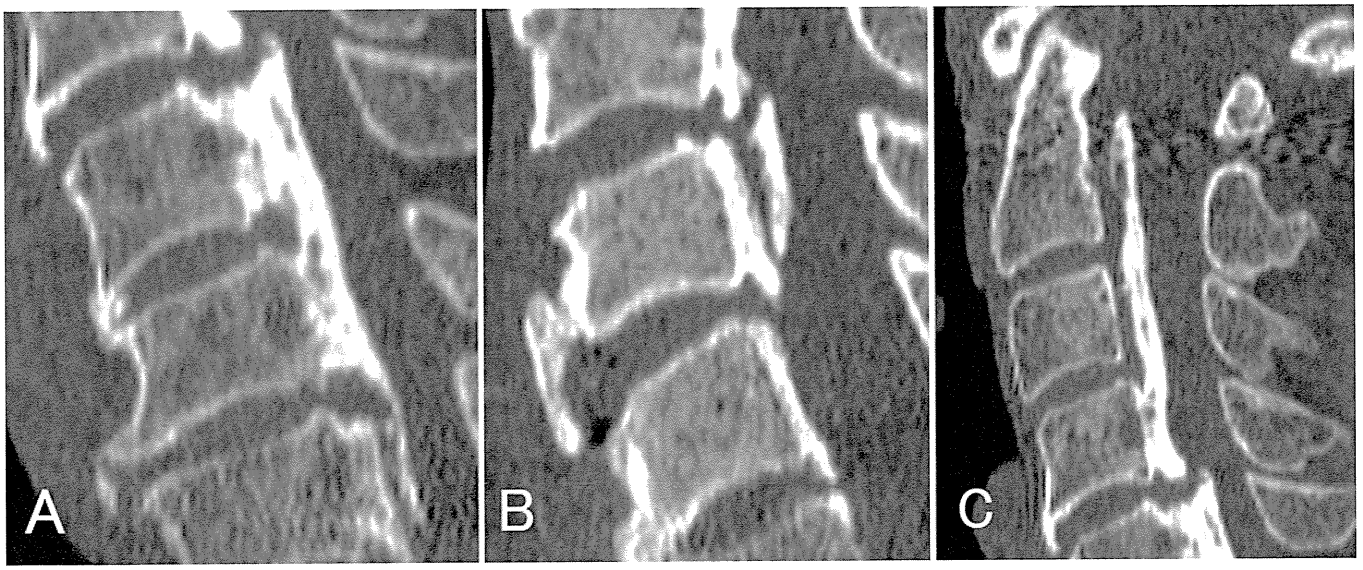

FIG. 3. Computed tomography scans showing the bridging **(A)**, nonbridging **(B)**, and stalagmite **(C)** types of ossification.

3D CT scanning revealed the discontinuity of ossifications in each intervertebral segment (Fig. 4). In fact, all ossifications in this patient were of the nonbridging type (Fig. 5). The intervertebral ROM in AP flexion and axial rotation was 6.5°and 10.2° at C3–C4, 7.7° and 3.4° at C4–5, 11.3° and 1.9° at C5–6, and 16.6° and 4.9° at C6–7.

Case 2

This 71-year-old man with continuous-type ossifications documented by plain radiographs had been treated conservatively with monitoring. The intervertebral ROM of AP flexion was 3.5° at C2–3, 0.9° at C3–4, 16.6° at C4–5, 13.8° at C5–6, and 13.5° at C6–7. The compensa-

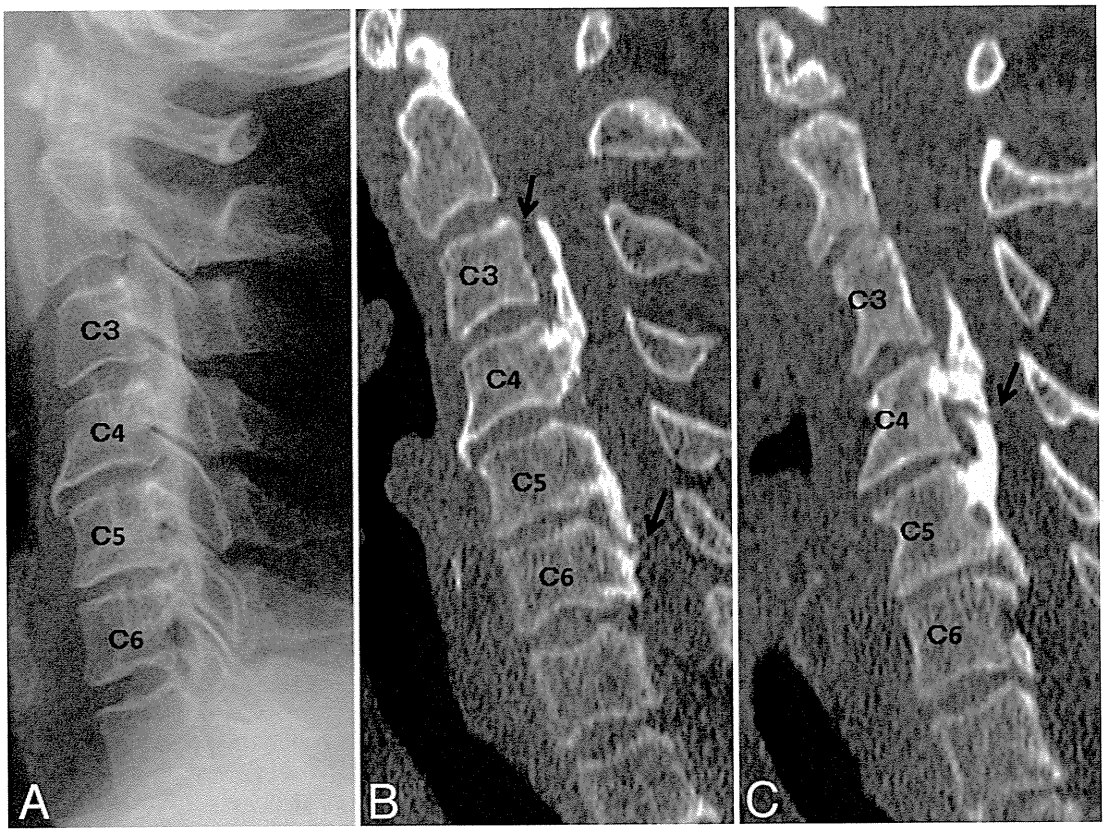

FIG. 4. Case 1. Radiograph **(A)** and CT scans **(B and C)** of ossifications. The radiograph shows a continuous-type OPLL at the C3–6 level; however, the reconstructed scans reveal the discontinuity *(arrows)* of ossifications of the nonbridging type.

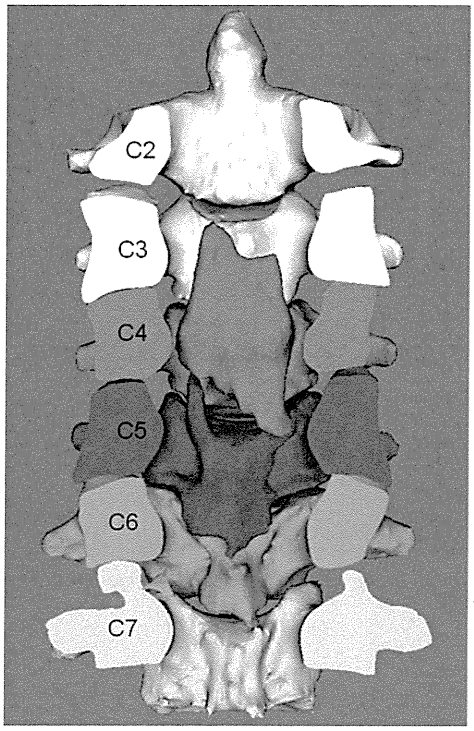

	AP flexion (°)	Rotation (°)
C2-3	8.3	2.9
C3-4	6.5	10.2
C4-5	7.7	3.4
C5-6	11.3	1.9
C6-7	16.6	4.9

FIG. 5. Case 1. Three-dimensional model, viewed from behind, of ossifications of the nonbridging type. The vertebral arches are removed for better visualization.

tory increase in ROM occurred in the adjacent intervertebral segment of C4–5. Unfortunately, the patient fell and sustained a spinal cord injury. Magnetic resonance imaging suggested that a stalagmite-type ossification hit the spinal cord like a lever, using the C4–5 mobile segment as a fulcrum point (Fig. 6).

Discussion

The 4-category classification system of the Japanese Investigation Committee on the Ossification of the Spinal Ligaments reported by Tsuyama[18] has long been the only radiographic classification system used for cervical OPLL (Fig. 1). Many studies have been performed using this classification. Matsunaga et al.[11] and Mochizuki et al.[14] reported that segmental or mixed-type ossification with a wide ROM was a risk factor for myelopathy compared with continuous-type ossification. Although the accurate quantification of intervertebral ROM has been difficult, continuous-type ossification has been considered to have fewer dynamic factors. It is true that continuous-type ossifications in our study had a comparatively small average ROM of 3.7° in AP flexion and 3.0° in axial rotation. However, the 4-category radiographic classification originally did not take dynamic factors into consideration. Actually, we found that in continuous-type ossifications, there was a marked difference in intervertebral ROM between bridging and nonbridging ossifications. These types of ossification were easily distinguishable on the basis of reconstructed sagittal CT scans. We demonstrated that on plain radiographs, 73% of continuous-type ossifications had discontinuity in some places and had 4.9° of AP flexional motion and 4.0° of rotation on average. Except for stalagmite-type ossifications, the nonbridging ossifications had as much as 5.6° of AP flexional motion. Only 27% of continuous-type ossifications corresponding to the bridging type had a little motion in the true sense. An earlier study found the prevalence of continuous-type and mixed-type ossifications on plain radiographs to be 27% and 29%, respectively;[18] however, the prevalence is different in 3D evaluation on 3D CT scans.[2,9] Chang et al.[2] reported the differences between 3D morphology on CT scans and the 4-category classification system using

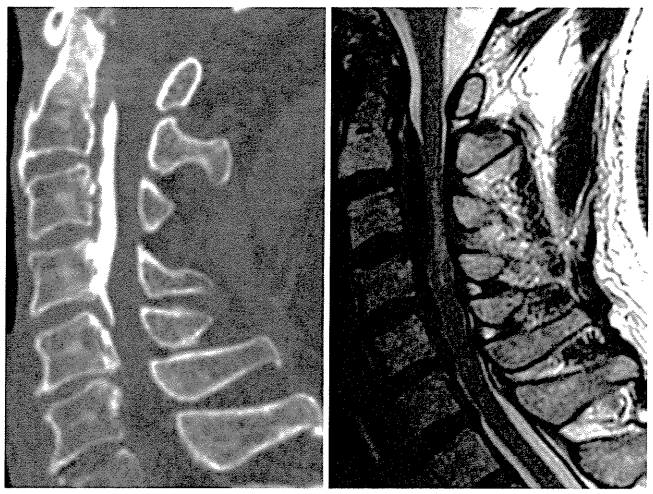

FIG. 6. Case 2. Computed tomography scan **(left)** and MRI study **(right)** of the cervical spine. The MRI study shows a T2 high-intensity area in the spinal cord at the C3–4 level.

radiographs. In their study, many continuous-type ossifications classified by radiography were reclassified as the mixed type in evaluation with CT. The kappa value of 3D CT classification was 0.86, much higher than that for radiographic classification. Kawaguchi et al.[9] also reported that 3D CT visualization provided more accurate information than radiography did. Our findings correspond with those of Chang et al. and Kawaguchi et al. Our results, which are based on 3D kinematics, could be a foundation for a new CT classification system for OPLL, one that includes dynamic factors. Further investigations of the relationship between the vertebral level responsible for myelopathy and the nonbridging-type segments will provide additional details about dynamic factors. As Fujiyoshi et al.[4] recommended, additional fusion for mobile segments in posterior decompression surgery to reduce dynamic factors may improve the prognosis. In determining the indications for additional fusion, assessment of bridging-type versus nonbridging-type ossifications can be useful.

Three-dimensional morphological evaluation also provided helpful anatomical information. Stalagmite-type ossifications had continuity of the ossification itself but were separated from the posterior wall of the upper vertebra. The long ossification originating from the lower vertebra extended behind throughout the length of the upper vertebra and was thought to block the upper vertebra so that it could not shift posteriorly. Therefore, the intervertebral segment of stalagmite-type ossifications had normal axial rotation but restricted AP flexion. We speculate that the reason this type of ossification existed only in the upper cervical spine derived from the anatomical morphology of the posterior longitudinal ligament. In the transitional process of the posterior longitudinal ligament to the tectorial membrane, the posterior longitudinal ligament may separate from the posterior wall of the vertebra by covering the transverse ligament behind the C-2 dens. Therefore, the ossification hardly attaches to the C-2 vertebra even when the posterior ligament ossifies. Interestingly, the original illustration of the radiographic classification system that appeared in the report by Tsuyama[18] observantly depicted the separation from the posterior wall of C-2 that is characteristic of continuous-type ossification (Fig. 1), although nothing was explained in the figure legends in that report.

Conclusions

Although ossification may seem to be of the continuous type on plain radiographs, the type actually comprises 2 kinds of ossification: 1) the bridging type, which has virtually no motion clinically; and 2) the nonbridging type, which has an average of 4.9° of AP flexion and 4.0° of rotation. The discrimination between bridging and nonbridging ossification on sagittal CT scans is a practical index for the existence of dynamic factors.

Disclosure

This work was supported by a grant-in-aid from the Investigation Committee on Ossification of the Spinal Ligaments, Japanese Ministry of Public Health, Labor, and Welfare, and a grant-in-aid for Scientific Research C (KAKENHI:22591632) from the Japan Society for the Promotion of Science. No benefits in any form have been or will be received from a commercial party related directly or indirectly to the subject of this manuscript. Our institution's review board approved the study reported in this manuscript.

Author contributions to the study and manuscript preparation include the following. Conception and design: Fujimori, Iwasaki. Acquisition of data: Fujimori. Analysis and interpretation of data: Fujimori, Nagamoto. Drafting the article: Fujimori. Critically revising the article: all authors. Reviewed submitted version of manuscript: all authors. Approved the final version of the manuscript on behalf of all authors: Fujimori. Statistical analysis: Fujimori. Administrative/technical/material support: Iwasaki, Sugamoto, Yoshikawa. Study supervision: Iwasaki.

Acknowledgments

The authors thank the Investigation Committee on the Ossification of the Spinal Ligaments of the Japanese Ministry of Health, Labor, and Welfare; and Scientific Research (C) from the Ministry of Education, Culture, Sports, Science, and Technology. Katharine O'Moore-Klopf, ELS (East Setauket, NY), provided professional English-language editing of this article.

References

1. Azuma Y, Kato Y, Taguchi T: Etiology of cervical myelopathy induced by ossification of the posterior longitudinal ligament: determining the responsible level of OPLL myelopathy by correlating static compression and dynamic factors. **J Spinal Disord Tech 23:**166–169, 2010
2. Chang H, Kong CG, Won HY, Kim JH, Park JB: Inter- and intra-observer variability of a cervical OPLL classification using reconstructed CT images. **Clin Orthop Surg 2:**8–12, 2010
3. Côté P, Cassidy JD, Yong-Hing K, Sibley J, Loewy J: Apophysial joint degeneration, disc degeneration, and sagittal curve of the cervical spine. Can they be measured reliably on radiographs? **Spine (Phila Pa 1976) 22:**859–864, 1997
4. Fujiyoshi T, Yamazaki M, Okawa A, Kawabe J, Hayashi K, Endo T, et al: Static versus dynamic factors for the development of myelopathy in patients with cervical ossification of the posterior longitudinal ligament. **J Clin Neurosci 17:**320–324, 2010
5. Harrison DE, Harrison DD, Cailliet R, Troyanovich SJ, Janik TJ, Holland B: Cobb method or Harrison posterior tangent method: which to choose for lateral cervical radiographic analysis. **Spine (Phila Pa 1976) 25:**2072–2078, 2000
6. Inoue S, Goto S, Nagase J, Tanaka Y: Investigation of window width and window level of computed tomography for OPLL, in **Annual Report of Taskforce of Research for Ossification of the Spinal Ligaments.** Tokyo: Japanese Ministry of Public health and Welfare, Vol 58, 1984, pp 237–239
7. Iwasaki M, Okuda S, Miyauchi A, Sakaura H, Mukai Y, Yonenobu K, et al: Surgical strategy for cervical myelopathy due to ossification of the posterior longitudinal ligament: Part 1: Clinical results and limitations of laminoplasty. **Spine (Phila Pa 1976) 32:**647–653, 2007
8. Iwasaki M, Okuda S, Miyauchi A, Sakaura H, Mukai Y, Yonenobu K, et al: Surgical strategy for cervical myelopathy due to ossification of the posterior longitudinal ligament. Part 2: Advantages of anterior decompression and fusion over laminoplasty. **Spine (Phila Pa 1976) 32:**654–660, 2007
9. Kawaguchi Y, Urushisaki A, Seki S, Hori T, Asanuma Y, Kimura T: Evaluation of ossification of the posterior longitudinal ligament by three-dimensional computed tomography and magnetic resonance imaging. **Spine J 11:**927–932, 2011

10. Liu T, Xu W, Cheng T, Yang HL: Anterior versus posterior surgery for multilevel cervical myelopathy, which one is better? A systematic review. **Eur Spine J 20:**224–235, 2011
11. Matsunaga S, Kukita M, Hayashi K, Shinkura R, Koriyama C, Sakou T, et al: Pathogenesis of myelopathy in patients with ossification of the posterior longitudinal ligament. **J Neurosurg 96 (2 Suppl):**168–172, 2002
12. Matsunaga S, Nakamura K, Seichi A, Yokoyama T, Toh S, Ichimura S, et al: Radiographic predictors for the development of myelopathy in patients with ossification of the posterior longitudinal ligament: a multicenter cohort study. **Spine (Phila Pa 1976) 33:**2648–2650, 2008
13. Matsunaga S, Sakou T, Taketomi E, Nakanisi K: Effects of strain distribution in the intervertebral discs on the progression of ossification of the posterior longitudinal ligaments. **Spine (Phila Pa 1976) 21:**184–189, 1996
14. Mochizuki M, Aiba A, Hashimoto M, Fujiyoshi T, Yamazaki M: Cervical myelopathy in patients with ossification of the posterior longitudinal ligament. Clinical article. **J Neurosurg Spine 10:**122–128, 2009
15. Morio Y, Nagashima H, Teshima R, Nawata K: Radiological pathogenesis of cervical myelopathy in 60 consecutive patients with cervical ossification of the posterior longitudinal ligament. **Spinal Cord 37:**853–857, 1999
16. Nagamoto Y, Ishii T, Sakaura H, Iwasaki M, Moritomo H, Kashii M, et al: In vivo three-dimensional kinematics of the cervical spine during head rotation in patients with cervical spondylosis. **Spine (Phila Pa 1976) 36:**778–783, 2011
17. Polly DW Jr, Kilkelly FX, McHale KA, Asplund LM, Mulligan M, Chang AS: Measurement of lumbar lordosis. Evaluation of intraobserver, interobserver, and technique variability. **Spine (Phila Pa 1976) 21:**1530–1536, 1996
18. Tsuyama N: Ossification of the posterior longitudinal ligament of the spine. **Clin Orthop Relat Res (184):**71–84, 1984

Manuscript submitted December 21, 2011.
Accepted March 12, 2012.
Please include this information when citing this paper: published online April 27, 2012; DOI: 10.3171/2012.3.SPINE111083.

Supplemental online information:

Video 1: http://mfile.akamai.com/21490/wmv/digitalwbc.download.akamai.com/21492/wm.digitalsource-na-regional/spine11-1083_video_1.asx (Media Player).
http://mfile.akamai.com/21488/mov/digitalwbc.download.akamai.com/21492/qt.digitalsource-global/spine11-1083_video_1.mov (Quicktime).
Video 2: http://mfile.akamai.com/21490/wmv/digitalwbc.download.akamai.com/21492/wm.digitalsource-na-regional/spine11-1083_video_2.asx (Media Player).
http://mfile.akamai.com/21488/mov/digitalwbc.download.akamai.com/21492/qt.digitalsource-global/spine11-1083_video_2.mov (Quicktime).
Video 3: http://mfile.akamai.com/21490/wmv/digitalwbc.download.akamai.com/21492/wm.digitalsource-na-regional/spine11-1083_video_3.asx (Media Player).
http://mfile.akamai.com/21488/mov/digitalwbc.download.akamai.com/21492/qt.digitalsource-global/spine11-1083_video_3.mov (Quicktime).

Address correspondence to: Takahito Fujimori, M.D., Department of Orthopedic Surgery, Osaka University Graduate School of Medicine, 2-2 Yamadaoka, Suita, Osaka 565-0871, Japan. email: takahito-f@hotmail.co.jp.

J Neurosurg Spine 17:327–333, 2012

Three-dimensional motion of the uncovertebral joint during head rotation

Clinical article

Yukitaka Nagamoto, M.D., Ph.D.,[1] Takahiro Ishii, M.D., Ph.D.,[2] Motoki Iwasaki, M.D., Ph.D.,[1] Hironobu Sakaura, M.D., Ph.D.,[3] Hisao Moritomo, M.D., Ph.D.,[1] Takahito Fujimori, M.D., Ph.D.,[1] Masafumi Kashii, M.D., Ph.D.,[1] Tsuyoshi Murase, M.D., Ph.D.,[1] Hideki Yoshikawa, M.D., Ph.D.,[1] and Kazuomi Sugamoto, M.D., Ph.D.[1]

[1]Department of Orthopaedics, Osaka University Graduate School of Medicine; [2]Department of Orthopaedic Surgery, Kaizuka City Hospital, Osaka; and [3]Department of Orthopaedic Surgery, Kansai Rosai Hospital, Hyogo, Japan

Object. The uncovertebral joints are peculiar but clinically important anatomical structures of the cervical vertebrae. In the aged or degenerative cervical spine, osteophytes arising from an uncovertebral joint can cause cervical radiculopathy, often necessitating decompression surgery. Although these joints are believed to bear some relationship to head rotation, how the uncovertebral joints work during head rotation remains unclear. The purpose of this study is to elucidate 3D motion of the uncovertebral joints during head rotation.

Methods. Study participants were 10 healthy volunteers who underwent 3D MRI of the cervical spine in 11 positions during head rotation: neutral (0°) and 15° increments to maximal head rotation on each side (left and right). Relative motions of the cervical spine were calculated by automatically superimposing a segmented 3D MR image of the vertebra in the neutral position over images of each position using the volume registration method. The 3D intervertebral motions of all 10 volunteers were standardized, and the 3D motion of uncovertebral joints was visualized on animations using data for the standardized motion. Inferred contact areas of uncovertebral joints were also calculated using a proximity mapping technique.

Results. The 3D animation of uncovertebral joints during head rotation showed that the joints alternate between contact and separation. Inferred contact areas of uncovertebral joints were situated directly lateral at the middle cervical spine and dorsolateral at the lower cervical spine. With increasing angle of rotation, inferred contact areas increased in the middle cervical spine, whereas areas in the lower cervical spine slightly decreased.

Conclusions. In this study, the 3D motions of uncovertebral joints during head rotation were depicted precisely for the first time.

(http://thejns.org/doi/abs/10.3171/2012.6.SPINE111104)

Key Words • **uncovertebral joint** • **three-dimensional kinematics** • **head rotation** • **volume registration** • **cervical**

The uncovertebral joints (Luschka joints) are small but clinically important anatomical structures of the cervical vertebrae. Each joint consists of the uncinate process and corresponding recess located on the inferolateral surface of the superior adjacent vertebral body. In the aged or degenerative cervical spine, osteophytes arising from an uncovertebral joint can cause cervical radiculopathy, often requiring decompression surgery. Although the biomechanical roles[1,13,18,19,24] and morphological characteristics[4,6,14,17] of the uncovertebral joints have been investigated, the functions of uncovertebral joints have yet to be definitively clarified. Full elucidation of the function, including kinematics, of the uncovertebral joints is thus very important.

According to previous comparative anatomical investigations, uncinate processes are found only in ob-

This article contains some figures that are displayed in color online but in black-and-white in the print edition.

ligate or facultative bipedal animals, such as primates, marsupials, and rodents.[7] In the upright position, rotation of the cervical spine is needed to allow the animal to look around. From this anatomical observation, uncovertebral joints are believed to play some role in head rotation.[17,19] To the best of our knowledge, however, no studies have reported kinematics of the uncovertebral joints during head rotation. We have developed a 3D imaging system to noninvasively evaluate relative motions of individual cervical vertebrae in vivo.[8–10] The purpose of this study was to elucidate 3D motion of the uncovertebral joints to provide a better understanding of the function of these joints during head rotation.

Methods

Study Population

Study participants were 10 healthy volunteers (5 men and 5 women) with neither neck pain nor a medical history of cervical spine disorders. Mean age at the time of imaging was 25.1 years (range 22–31 years). All study protocols were approved by the institutional review board. Informed consent was obtained in all volunteers.

Acquisition of 3D MRI

Each volunteer was placed supine on the MRI table and underwent 3D MRI in 11 positions with the head rotated: 0° (neutral), 15°, 30°, 45°, and 60°, and maximum rotation to each side (left and right). We instructed all volunteers to rotate the head as perpendicularly as possible about the axis of the body trunk. The shoulders of each volunteer were fixed to the table using a band. All 3D MRI scans were acquired using a 1.0-T commercial MRI system (Signa LX, General Electric) in conjunction with a torso-phased array coil. A 3D fast-gradient recalled acquisition in the steady state (GRASS) sequence was used (TR 8.0 msec, TE 3.3 msec, slice thickness 1.5 mm, no interslice gap, flip angle 10°, FOV 24 cm, inplane acquisition matrix 256 × 224). Magnetic resonance imaging data were saved in DICOM format and transmitted to a computer workstation, where image processing was performed using software developed in our laboratory (Virtual Place M series, Medical Imaging Laboratory).

Motion Analysis

Our original method used in the present study has been fully described in previous reports[8–10] and will be described here only briefly. First, regions of interest were extracted in 3D from the 3D MRI data (segmentation) and 6 vertebrae from C-2 to C-7 were extracted semiautomatically using an intensity threshold technique. Second, using a volume registration method,[8–10] 3D motions of each vertebra in an absolute coordinate system were calculated by automatically superimposing the segmented region of each vertebra on 3D MRI in the neutral position over images of every position. Intervertebral motions of every motion segment from C2–3 to C6–7 were then calculated by converting the absolute motion (3 × 4 matrix) obtained from the preceding image processing into a relative motion with respect to the subjacent vertebra. These motions were expressed in 6 df by Euler angles with the sequence of pitch (X), yaw (Y), roll (Z), and translations using a previously defined anatomical coordinate system.[8–10] Accuracy of this method was as follows: 0.24° for flexion-extension, 0.31° for lateral bending, 0.43° for axial rotation, 0.52 mm for superoinferior translation, 0.51 mm for anteroposterior translation, and 0.41 mm for lateral translation, as described in detail previously.[10]

Creation of 3D Bone Models

Surface bone models constructed from 3D MRI data provided insufficient information on configuration to investigate in vivo 3D kinematics of the uncovertebral joint, due to a lack of spatial resolution. We therefore decided to choose surface bone models from multidetector row CT (LightSpeed 16, General Electric) for analysis, and these models reproduced anatomical structures much more accurately than models from 3D MRI. Computed tomography data for the cervical spine were selected from the DICOM server at our institution, based on anatomical characteristics described in several studies of the uncovertebral joints.[4,6,14,17,18] The source of the data was a 28-year-old man who was not part of the 10-patient cohort. More specifically, characteristics of the selected CT data were as follows: the uncinate processes situated laterally at middle cervical levels (C2–3, C3–4, C4–5) and dorsolaterally at lower cervical levels (C5–6, C6–7)[6,17] demonstrated reduced height of the processes in relation to the vertebral bodies at lower cervical levels (Fig. 1).[4,14] Regarding sagittal orientation of facets, facet slope is more gradual as the cervical level descends caudally. There were no degenerative changes, and normal disc heights were maintained at all levels on conventional 2D MRI. In this way, 6 surface bone models from C-2 to C-7 were created.

Three-Dimensional Visualization of Motion

All intervertebral motions from the 10 volunteers were aggregated and standardized at every intervertebral level using our original operation algorithm. The results of standardized 3D intervertebral motions were expressed as matrices. A pair of CT vertebral models of a functional spinal unit was displayed in virtual 3D space, allowing us to obtain a 3D movie of intervertebral motions by introducing the matrices to the superior adjacent vertebra alone and keeping the subjacent vertebra fixed (Fig. 2, Video 1).

Video 1. Clip showing 3D motion of the uncovertebral joints. This 3D animation of the uncovertebral joints during head rotation shows joints alternating between contact and separation accompanying torsion of the intervertebral space. To allow a better understanding of intervertebral motions, the subjacent vertebra is always fixed in this clip. For example, C-3 is fixed in the clip showing C2–3. Click here to view with Media Player. Click here to view with Quicktime.

Creation of the animation was accomplished using originally developed software (Orthopedics Viewer, Osaka University) that allowed the observer to closely examine every uncovertebral joint from every observation point needed. These 3D animations helped us to better understand the joint kinematics.

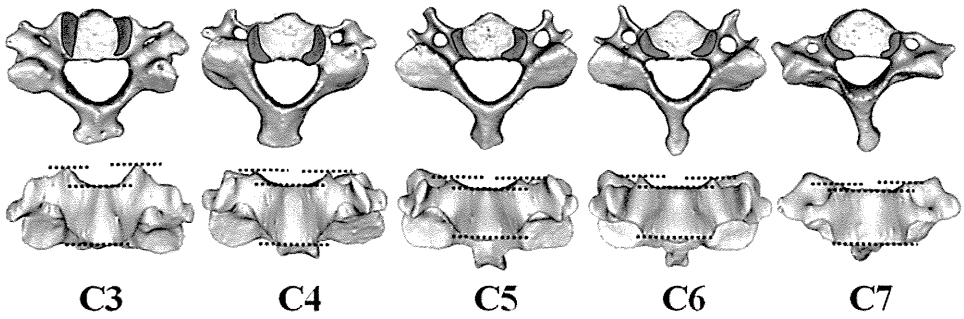

FIG. 1. Surface bone models created using CT data. We chose CT data with the following anatomical characteristics: uncinate processes situated laterally at middle cervical levels (C3–4) and dorsolaterally at lower cervical levels (C5–7), represented in the **upper** row as *dark gray* areas, as well as relatively reduced height of the processes at lower cervical levels, represented in the **lower** row as *dashed lines*.

Contact Area

We measured inferred contact areas of the uncovertebral joints during head rotation from bone surface models using a proximity mapping method.[16] Proximity mapping involves the visualization of distance from 1 bone to the nearest neighboring bone. We defined the area within a preset interbone distance as the inferred contact area. Contact areas were investigated at 15° increments during head rotation at every intervertebral level from C2–3 to C6–7 (Fig. 3, Video 2).

VIDEO 2. Clip showing inferred contact area of the uncovertebral joint. The inferred contact areas of the uncinate processes during head rotation were situated directly lateral at the middle cervical spine and dorsolateral at the lower cervical spine. Click here to view with Media Player. Click here to view with Quicktime.

Thresholds of preset interbone distances varied within 0.5–1.0 mm according to the individual joint size and intervertebral space.

Results

Intervertebral Motion

In main axial rotation, C4–5 and C5–6 were the most mobile segments and C2–3 was the least mobile segment, as previously reported (Table 1). During head rotation, larger rotation angles were observed in coupled lateral bending than in main axial rotation in all segments, and C2–3 and C3–4 were the most mobile segments in coupled lateral bending, despite the immobility in axial rotation (Table 2).

Behavior of Uncovertebral Joints

The 3D animation of uncovertebral joints during head rotation showed joints alternating between contact and separation accompanying torsion of the intervertebral space. On the side ipsilateral to head rotation, both joint surfaces were in contact with each other, while those on the contralateral side were separated (Fig. 2, Video

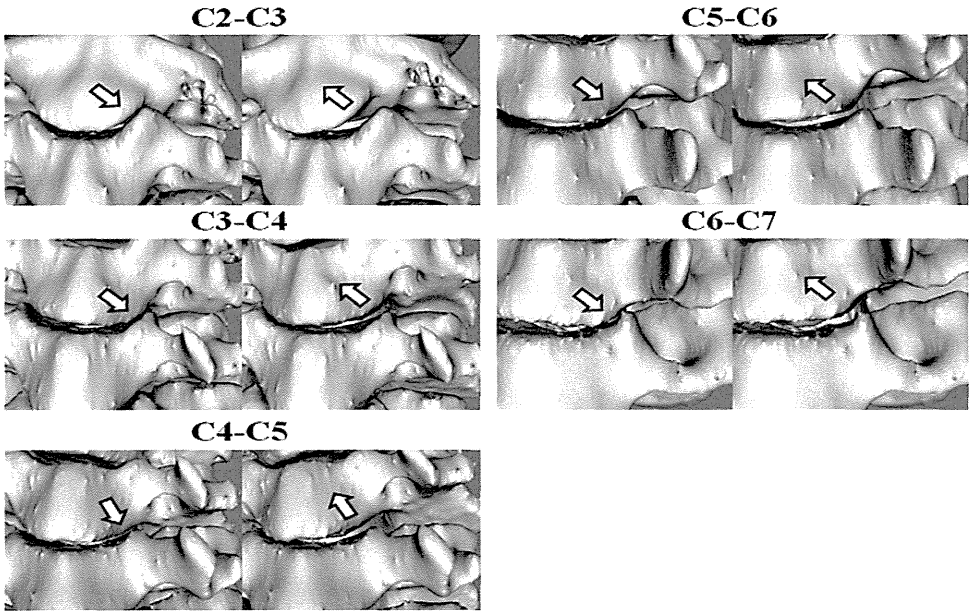

FIG. 2. The behaviors of uncovertebral joints were shown in a 3D animation. Each paired image focuses on the left uncovertebral joint from a left anterior oblique view. *Downward arrows* show contact and *upward arrows* show separation of the joint. For each level, left panels represent head rotation to the left, and right panels represent head rotation to the right.

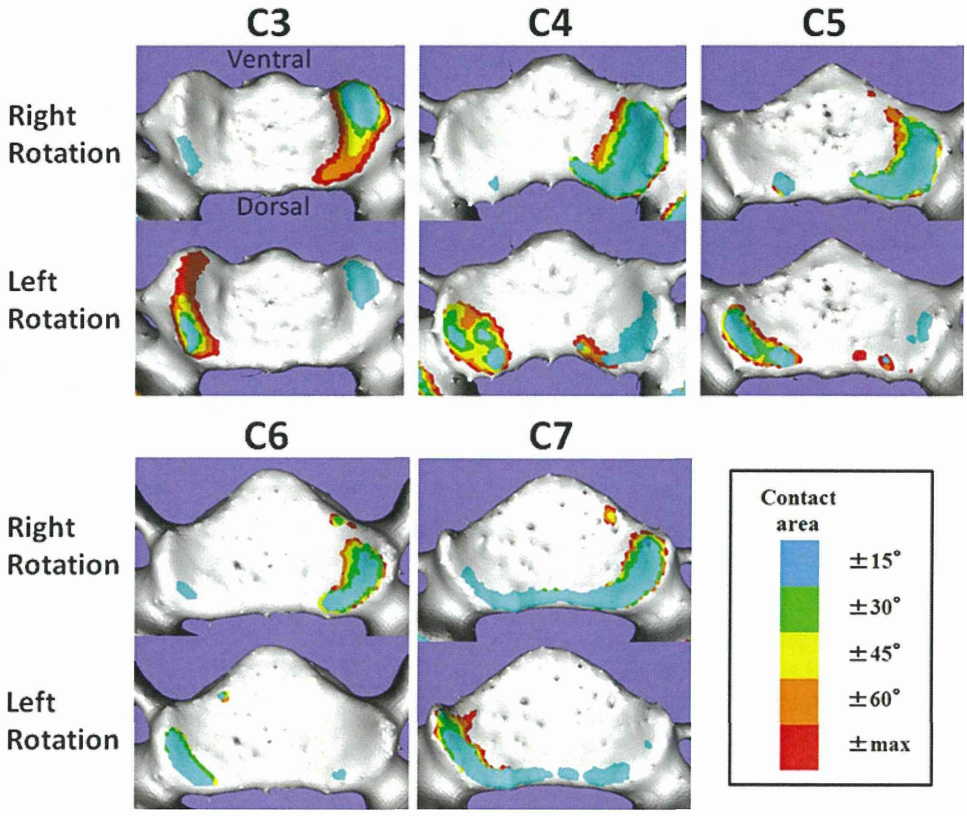

FIG. 3. Inferred contact areas projected on the uncinate process side. Each panel represents a cranial view with the upper part of each panel as the ventral side. Inferred contact areas are shown using 5 different colors, as shown in the **key**.

1). This pattern of motion was strongly apparent in the middle cervical spine, especially at the C2–3 level.

Contact Areas for Uncovertebral Joints

Inferred contact areas of the uncovertebral joints are shown in Fig. 3 and Video 2. Inferred contact areas showed that the uncovertebral joints were the first contact areas in the intervertebral space during head rotation and were situated directly lateral at the middle cervical spine and dorsolateral at the lower cervical spine. The dimensions (mm^2) of inferred contact areas were also calculated (Fig. 4). With increasing rotation angle of the head, inferred contact areas increased in the middle cervical spine, but slightly decreased in the lower cervical spine.

Discussion

Roles for Uncovertebral Joints and Uncinate Processes During Head Rotation

During head rotation, lateral flexion is coupled with rotation in the cervical spine and is called "coupled motion." Facet joints undoubtedly represent the biggest contributors to such motion, due to their oblique orientation.[9,18] In addition, several studies have suggested the contribution

TABLE 1: Intervertebral motion during head rotation: main axial rotation*

Head Rotation Angle (°)	C2–3	C3–4	C4–5	C5–6	C6–7
rt max	−2.3 ± 1.2	−4.7 ± 1.0	−4.9 ± 1.3	−4.5 ± 0.8	−2.6 ± 0.7
rt 60	−1.5 ± 0.9	−3.6 ± 0.8	−4.0 ± 1.2	−3.8 ± 0.6	−2.3 ± 0.5
rt 45	−0.7 ± 0.8	−2.3 ± 0.5	−2.7 ± 1.3	−2.9 ± 0.4	−2.0 ± 0.8
rt 30	−0.2 ± 0.7	−1.0 ± 0.7	−1.7 ± 1.1	−1.9 ± 0.7	−1.2 ± 0.9
rt 15	0.0 ± 0.7	−0.2 ± 0.5	−0.8 ± 0.5	−1.3 ± 0.7	−1.0 ± 0.9
lt 15	−0.4 ± 0.6	0.2 ± 0.7	0.9 ± 0.5	1.6 ± 1.2	0.7 ± 1.1
lt 30	0.2 ± 0.4	1.1 ± 0.9	1.4 ± 0.5	1.8 ± 1.4	1.0 ± 1.4
lt 45	0.4 ± 0.5	2.0 ± 0.9	2.1 ± 0.7	2.4 ± 1.4	1.2 ± 0.9
lt 60	1.1 ± 0.7	2.9 ± 1.0	3.1 ± 0.9	3.3 ± 1.5	2.1 ± 1.0
lt max	1.5 ± 0.6	3.8 ± 1.0	3.9 ± 1.1	4.0 ± 1.5	2.4 ± 0.9

* All values given in mean degrees ± SD. Negative values = right axial rotation; positive values = left axial rotation.

TABLE 2: Intervertebral motion during head rotation: coupled lateral bending*

Head Rotation Angle (°)	C2–3	C3–4	C4–5	C5–6	C6–7
rt max	4.0 ± 1.3	6.2 ± 1.1	5.7 ± 1.1	5.6 ± 1.2	4.9 ± 1.8
rt 60	2.5 ± 1.3	5.0 ± 1.2	4.4 ± 1.3	4.9 ± 1.1	3.6 ± 1.4
rt 45	0.6 ± 1.0	3.1 ± 1.2	3.5 ± 1.2	3.0 ± 1.2	2.5 ± 1.7
rt 30	−0.6 ± 1.7	1.8 ± 1.2	1.9 ± 1.0	2.4 ± 1.3	1.7 ± 1.9
rt 15	−0.9 ± 1.6	0.7 ± 0.9	1.3 ± 0.8	1.2 ± 1.5	1.3 ± 1.2
lt 15	1.4 ± 2.1	−0.4 ± 0.9	−1.7 ± 1.3	−1.2 ± 1.3	−1.6 ± 2.7
lt 30	0.4 ± 2.0	−1.4 ± 0.8	−1.6 ± 1.1	−2.2 ± 1.9	−1.2 ± 1.9
lt 45	−0.8 ± 2.2	−2.3 ± 0.8	−2.6 ± 0.8	−2.6 ± 1.7	−2.5 ± 2.0
lt 60	−2.0 ± 2.1	−3.7 ± 1.2	−3.7 ± 0.7	−3.7 ± 1.3	−3.1 ± 2.3
lt max	−3.5 ± 1.8	−5.0 ± 1.2	−4.8 ± 1.0	−4.6 ± 1.4	−4.3 ± 2.2

* All values given in mean degrees ± SD. Negative values = left lateral bending; positive values = right lateral bending.

of uncinate processes to coupled motion.[1,7,18,19] Hall[7] noted that among vertebrates, uncinate processes on the cervical vertebrae are found only in obligate or facultative bipeds, which require rotation of the neck to look around. Given these findings, he hypothesized that the uncovertebral joints arose during evolution from quadrupedalism to bipedalism, and bear some relationship to neck rotation. To verify Hall's hypothesis, Penning and Wilmink[19] calculated the axis of rotation from the anatomical shape of uncovertebral joints, using CT sections in the plane of the facet joints in 2 different positions. These authors showed that coupling of lateral bending and rotation of the middle and lower cervical spine might be explained exclusively by the axis and morphological structure of the uncovertebral joints, and that the uncinate processes are also essential for rotation. Clausen et al.[1] quantitatively investigated contributions of the uncovertebral joints to motion of a spinal segment, including axial rotation, for the first time. Using finite element models, they elucidated that the presence of the uncovertebral joint (a fissure) leads to increased motions, while the uncinate processes act as stabilizers with respect to motion of the cervical spinal segment, particularly during axial rotation and lateral bending of the cervical spine.[1] However, that study was performed using only computer simulations, and the acquired data were not derived from real sources. Moreover, they analyzed kinematics only at the C5–6 segment, whereas anatomical variations at different vertebral levels may influence cervical biomechanics.

In our study, with increasing angle of head rotation, two opposite surfaces of the uncovertebral joint became closer and closer on the ipsilateral side of rotation, while surfaces on the contralateral side became more and more separated. This pattern was strongly observed in the middle cervical spine. Moreover, at these levels, inferred contact areas were situated directly lateral and increased with increasing angle of rotation, particularly at C2–3. In the middle cervical spine, larger coupled lateral bending would accompany head rotation, as these levels show a steeper sagittal inclination of facets than those of the lower cervical spine.[11] Taking these findings together, we speculated that the presence of large processes relative to the vertebral body[14] might restrict excessive coupled lateral bending and disperse mechanical stresses effectively on large joint surfaces in the middle cervical spine. In fact, the C2–3 segment, which has the largest uncinate process, had the smallest motion in terms of both main axial rotation and coupled lateral bending in our study.

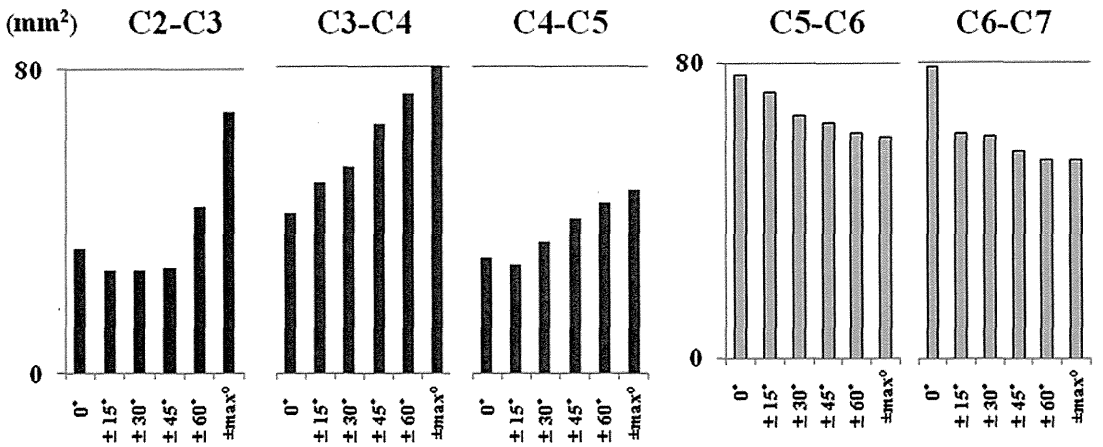

FIG. 4. Inferred contact areas (mm²) shown as means of right and left rotation at each intervertebral level, according to the angle of head rotation. With increasing rotation angle of the head, inferred contact areas increased in the middle cervical spine, but slightly decreased in the lower cervical spine.

Conversely, in the lower cervical spine, the inferred contact areas were situated dorsolaterally and these areas slightly decreased with increasing angle of rotation. Focusing only on the shape of the uncinate processes in the lower cervical spine, which displays more gradual inclination of facets than those of the middle cervical spine, axial rotation should be allowed without large coupled lateral bending. Therefore, the uncinate processes of the lower cervical spine might play a less important role in restricting excessive coupled lateral bending than those of the middle cervical spine. Given this observation, we speculated that uncinate processes of the lower cervical spine might not have to be as large as those of the middle cervical spine and instead play an important role in facilitating rotation of the cervical spine by placing the stress-focusing region on the posterolateral side of the upper surfaces of the vertebrae.

Nerve Root Compression and Uncovertebral Osteophytes in the Lower Cervical Spine

Cervical radiculopathy is often related to osteophyte formation around the uncinate process; C-7 root lesions are the most common, followed by C-6 lesions.[20,21] A longer course of the nerve root in close proximity to the uncovertebral joint may explain the predisposition toward nerve root compression by uncovertebral osteophytes at these levels.[3] However, anatomical or biomechanical reasons for a predisposition toward uncovertebral osteophytes in the lower cervical spine remain unclear.

In the present study, we elucidated that the uncovertebral joints are the first contact areas in the intervertebral space during head rotation. From these results, we speculated that as disc height diminishes with degeneration, earlier contact should occur around the uncovertebral joints during head rotation, and would be likely to promote age-related degenerative change around the uncovertebral joints due to the increased frequency of mechanical stress. If the degenerated disc causes abnormal intervertebral kinematics, further degenerative changes around the uncovertebral joints would occur. The lower cervical spine is well-known as the level most commonly affected by aging,[2,5,15,22] and moreover, inferred contact areas of the uncovertebral joints at the lower cervical spine were situated dorsolaterally and decreased with increasing angle of rotation. These contact areas are closer to the course of the nerve root than in the middle cervical spine and may be subjected to strong mechanical stress, because stresses are focused in such small areas. The accumulation of mechanical stress in joints induces osteophyte formation.[12] Head axial rotation movements are often repeated during activities of daily living.[23] Repeated head rotation in the course of activities of daily living might thus contribute to spur formation around contact areas of the uncovertebral joints in the lower cervical spine close to the intervertebral foramen. This speculative situation would account for the fact that cervical radiculopathy generally occurs in the lower cervical spine, particularly C5–6 and C6–7.

Limitations of the Study

Several limitations in this study must be addressed. First, information was obtained from animations (Videos 1 and 2) comprising only 11 different positions and could not be obtained with the volunteer in an upright position. Second, individual variability in uncovertebral joints6 could not be taken into account, even though these variations are likely to affect kinematics. Moreover, the surface bone models were constructed using data from a volunteer outside the 10-patient cohort. We acknowledge that this method includes the potential for bias. Third, contact areas of the uncovertebral joints were not "true" (verified), but were instead inferred. The presence of intervening tissues such as discs, joint cartilages, and synovial fluids were not taken into account. And fourth, contact pressure and pressure distributions could not be measured using our methods. Despite all these limitations, we believe that no other approaches currently allow the investigation of 3D motion of the uncovertebral joints in healthy individuals. The present study thus offers a step toward a better understanding of functions of the uncovertebral joints.

Conclusions

We have shown 3D motion of the uncovertebral joints during head rotation for the first time. Standardized 3D intervertebral motions of the cervical spine showed that the uncovertebral joints alternate between contact and separation during head rotation. Inferred contact areas of uncovertebral joints were situated directly lateral at the middle cervical spine and dorsolateral at the lower spine. With increasing angles of rotation, inferred contact areas increase in the middle cervical spine, particularly at C2–3, whereas areas slightly decrease in the lower cervical spine.

Disclosure

The authors report no conflict of interest concerning the materials or methods used in this study or the findings specified in this paper.

Author contributions to the study and manuscript preparation include the following. Conception and design: Nagamoto, Iwasaki, Moritomo. Acquisition of data: Nagamoto, Ishii. Analysis and interpretation of data: Nagamoto, Sakaura. Drafting the article: Nagamoto. Critically revising the article: all authors. Reviewed submitted version of manuscript: all authors. Approved the final version of the manuscript on behalf of all authors: Nagamoto. Administrative/technical/material support: Iwasaki, Murase, Yoshikawa, Sugamoto. Study supervision: Iwasaki, Murase, Yoshikawa, Sugamoto.

Acknowledgments

The authors thank Ryoji Nakao for assisting with software programming and Yoshihiro Sakaguchi for help with MRI.

References

1. Clausen JD, Goel VK, Traynelis VC, Scifert J: Uncinate processes and Luschka joints influence the biomechanics of the cervical spine: quantification using a finite element model of the C5-C6 segment. **J Orthop Res 15:**342–347, 1997
2. Dvorak J, Panjabi MM, Grob D, Novotny JE, Antinnes JA: Clinical validation of functional flexion/extension radiographs of the cervical spine. **Spine (Phila Pa 1976) 18:**120–127, 1993
3. Ebraheim NA, Lu J, Biyani A, Brown JA, Yeasting RA: